



Investigation of Drilling Performances, Tribological and Mechanical Behaviors of GFRC Filled with B₄C and Gr

Hüseyin Gürbüz¹ · İbrahim Halil Akcan¹ · Şehmus Baday¹ · Mehmet Emin Demir²

Received: 24 January 2024 / Accepted: 18 July 2024
© The Author(s) 2024

Abstract

In this study, the effects of Gr and B₄C filler materials on drilling performance, mechanical, and tribological behaviors of glass fiber-reinforced epoxy composites were experimentally investigated. Glass fiber-reinforced composite materials filled with B₄C and Gr at different weight ratios (5%, 10%, and 15%) were manufactured using hand lay-up method. The produced composite materials underwent various tests, including mechanical tests (tensile and flexural tests), tribological tests (wear behavior), and drilling tests under different parameters. Additionally, SEM images of the worn and fractured surfaces were examined. The addition of both B₄C and Gr fillers adversely affected the mechanical properties of glass fiber-reinforced composites. It was observed that tensile and flexural strengths decreased with increasing filler ratios. However, the addition of B₄C and Gr fillers enhanced the wear resistance of glass fiber-reinforced composites. It was revealed that in drilling operations, as the feed rate increased, the thrust forces increased, while the cutting speed increased, the thrust forces decreased. It was determined that delamination values in glass fiber reinforced composites decreased as the feed rate increase, while delamination values increased as the cutting speed increased. Generally, the thrust forces, vibration, delamination, and moment values obtained during the drilling of B₄C-filled glass fiber composites were found to be higher compared to Gr-filled glass fiber composites.

Keywords Epoxy composite · B₄C · Gr · Glass fiber · Drilling · Wear · Mechanical properties

1 Introduction

Polymers are frequently preferred in engineering applications due to their high thermal and mechanical properties, good adhesion to reinforcing materials, high chemical inertness, self-lubricating properties, low density, resistance to moisture and fatigue, ease of processing, and vibration

absorption [1–4]. However, low thermal conductivity of polymer matrix, high linear expansion rates, and low mechanical properties limit their use in certain applications [3]. One common method to enhance the properties of polymeric materials under different conditions is to reinforce polymers with different types of fibers and fillers [5–7]. In these composites, the polymer holds fibers and fillers together, ensuring even distribution of the load to the fibers and fillers [8, 9]. Resin, a type of polymers, is extensively used in production of fiber-reinforced composites due to its high wetting ability and adhesion to fibers, low shrinkage, easy manufacturing, and good electrical properties [10–12].

Fiber-reinforced epoxy matrix composites are gaining increasing popularity as alternatives to metal materials in marine vehicles, automotive, aircraft, defense, and chemical industries [13–17]. The use of filler materials in fiber-reinforced epoxy composites enhances various properties of these composites [18, 19]. Depending on the type, size, shape, and volume of the added filler particles, many properties of filled composites, such as mechanical (tensile, compressive, flexural, toughness, impact, etc.), tribological, thermal,

✉ Hüseyin Gürbüz
huseyin.gurbuz@batman.edu.tr

İbrahim Halil Akcan
ibrhmakcan1@gmail.com

Şehmus Baday
sehmus.baday@batman.edu.tr

Mehmet Emin Demir
memin.demir@batman.edu.tr

¹ Mechanical Engineering Department, Batman University, Batman, Turkey

² Beşiri Organized Industrial Zone Vocational School, Batman University, Batman, Turkey



Table 1 Some researches including different fibers and fillers type

Fiber and filler type	Ratio of filler	Consequences	Reference
Carbon, Al ₂ O ₃ , MoS ₂	5, 10%	Increased hardness and improved wear resistance	26
Glass and bamboo fibers, TiO ₂ , ZrO ₂	3, 6, 9%	Decreased erosion rate, tensile and flexural strength	27
Glass fiber, Al ₂ O ₃ , Gr	5%	Both filler increased tensile strength and hardness, Al ₂ O ₃ developed and Gr deteriorated wear resistance	28
Glass fiber, PTW, Gr	7.5% PTW, 2.5% Gr	Both filler decreased tensile and flexural strength, increased hardness and tribological properties	29
Glass fiber, SiC, Gr	5, 10% SiC, 5% Gr	Developed wear resistance, but lower rate of SiC was more effective	30
Glass fiber, SiC, Gr	5, 10%	Both filler improved tensile and flexural strength but decreased impact strength	6

and processability, can be modified [20, 21]. Researchers have investigated the effects of inorganic filler materials such as boron carbide (B₄C), graphite (Gr), alumina (Al₂O₃), graphene, SiO₂, TiO₂ on fiber-reinforced composites to produce new materials that can meet various needs [5, 6, 22–25]. Studies on different types of fibers and fillers conducted by some researchers are provided in Table 1.

Many researchers have reported that different types and ratios of fillers alter the mechanical, physical, and wear behaviour of reinforced composites. Raju et al. investigated the mechanical and wear behaviours of glass fiber-reinforced epoxy composites (GFRC) by adding Al₂O₃ filler in three different ratios. They observed an increase in tensile strength and modulus with Al₂O₃ reinforcement. It was noted that density and hardness increased with increasing filler ratios. They observed that the wear volume was higher in unfilled composites compared to filled composites, and they found that an increase in filler ratio reduced the wear volume [19].

Suresha et al. investigated wear behaviour and mechanical properties of SiC-filled GFRP composites. They found that SiC reinforcement increased the density, hardness, tensile and flexural strength of the composite. Additionally, they found that filled composites exhibited higher tribological performance compared to unfilled composites. They emphasized that increasing the load and sliding distance led to a greater mass loss and coefficient of friction. [26]. Hulgappa et al. investigated the flexural, tensile and impact strength of SiC and Gr-filled GFRP. They found that the addition of filler improved the mechanical properties of the GFRP [6]. Nayak et al. examined the effects of 10% Al₂O₃, SiO₂, and TiO₂ fillers in GFRP composites on the mechanical properties, hardness, and glass transition temperature. They determined that SiO₂ filler increased flexural strength, while Al₂O₃ increased hardness to a greater extent [27]. Zal et al., reported that the effect of fiber orientation angle on tensile, bending and impact strengths of glass fiber and stainless steel fibers was examined. They emphasized that the highest tensile stress of composite was obtained arranged at 0°. In their SEM analysis, it was stated that good adhesion was achieved between the fiber layers [28]. Rahmani et al., examined the hardness and wear behavior of epoxy matrix glass, carbon and kevlar reinforced composites. They stated that the hardness of carbon fiber reinforced composites was higher than glass and kevlar reinforced composites. They also revealed that the lowest wear rates were in Carbon, Glass and Kevlar reinforced composites, respectively [29]. In the study conducted by Hashemi et al., they investigated the effects of temperature, time and pressure on the mechanical properties of metal and glass reinforced composites. The best tensile and bending strength was obtained at 2.5 MPa pressure at 180° for 20 min. Based on SEM analysis, they revealed that the best adhesion and impregnation of glass and metal fibers was achieved at 180° [30]. Zhang compiled studies on the mechanical properties, surface characteristics, tribological behavior, and tribochemical reactions of SiC-reinforced composites under lubrication conditions. He also aims to enhance the understanding of wear mechanisms by offering recommendations for the design of low-wear SiC-reinforced composites in lubricated environments [31]. In engineering, ceramics are frequently utilized as tribological elements. Particularly, tribological materials composed of metal and ceramics are extensively used in various engineering applications such as piston rings, cylinder liners, engine cams, and many others. Boron carbide (B₄C), being the third hardest material, emerges as a suitable candidate for the production of components exposed to wear due to its superior properties such as high wear resistance, low density, high strength, and chemical inertness [32].

GFRC parts are connected to each other through fasteners, as in most applications. A large number of holes are needed

for connections that help mechanically join these composite materials. For example, approximately 55,000 holes are needed to build an Airbus A350 aircraft [33]. Therefore, it is of great importance to investigate the drilling parameters of these composites under appropriate machining and cutting conditions. Studies on drilling GFRPs are summarized below. Lukacs et al. determined the delaminations resulting from the drilling of GFRP using the image processing method. In their study, they found that the delamination values measured manually and the values measured by the image processing method were very close to each other. Therefore, they stated that this method could be used in delamination measurements [34]. Elwahed modelled and optimized the machining parameters using ANN in drilling GFRP with different thicknesses. It was found that the optimum machining parameters were cutting speed 1600 rpm and feed 0.025 mm/rev for a GFRP with a thickness of 5.4 mm. It was determined that the results of the ANN models applied to estimate the machining parameters are in agreement with the experimental results [35]. Khashaba et al. examined the heat-affected zone in drilling GFRP with different thicknesses and analysed the experimental results. In their study, they found that as the thickness of GFRP increased, the heat-affected zone increased significantly. They found that thrust force and cutting temperature together had a significant effect on delamination rates. They also explained the decrease in thrust force as the drilling time increases due to the increase in temperature [36]. Liu et al. examined the thrust force and delamination values in drilling GFRP with candlestick drills. Based on their results, they found that thrust force and delamination values decreased when appropriate geometric angles were formed [37]. Jessy et al. investigated the effect of different cooling methods on drill temperature in drilling GFRP. They found that the internal cooling method significantly reduced the drill temperature compared to other methods. They also revealed that the internal cooling method has significant contributions to reducing flank wear and increasing tool life [38]. Tian et al. examined the delamination and thrust forces resulting from drilling GFRP with candlestick drills. They found that the temperature decreased when the clearance angle of candlestick drill increased from 250 to 350. They found that as the feed rate increased, the amount of delamination decreased and the thrust force increased. They also found that as the cutting speed increased, the feed force decreased and the amount of delamination increased [39]. Erturk et al. investigated the effect of machining parameters and cutting temperature on drilling GFRP composites. They found that the optimum machining parameters were drill type HSS-TiN, cutting speed 2425 rpm and feed 0.13 mm/rev. They found that HSS-R drill had a significant effect on cutting temperature, while the cutting speed and feed had a minor contribution [40]. Mohan et al. investigated the effect of cutting parameters on thrust force and torque in drilling GFRP.

The optimum machining parameters for thrust force and torque were determined as feed rate 50 mm/min, workpiece thickness 3 mm, cutting speed 1500 rpm and drill diameter 3 mm [41]. Khashaba et al. performed a drilling analysis of GFRP. The authors found that high feed and cutting speed increased the amount of delamination, and wear on the drill caused the feed rate to increase [42]. Natarajan et al. examined the experimental results obtained in drilling GFRP. The authors stated that delamination values decreased due to the decreasing thrust force with increasing point angle (from 80° to 120°), which provides better surface quality with minimum tool wear [43].

In the study, mechanical, tribological and hole drilling parameters of GFRC materials produced using three different weight ratios (5, 10, 15%) and two different filler types (B₄C and Gr) were examined. As a result of the literature research, no comprehensive mechanical, tribological and hole-drilling studies of GFRC were found. With this study, both mechanical, tribological and hole-drilling problems of GFRC, which has a wide usage area in the field, but has some drilling problems, have been examined comprehensively, so the research results will be especially helpful to those who will work in this field.

2 Materials and Methods

2.1 Material

The structure of the glass fiber fabric (90°) used in the experiments is woven glass fiber and has a plain weave. The reinforcement types in the matrix material are B₄C and Gr. The glass fiber was obtained from Karbomid company, and B₄C and Gr powders were purchased from Ege Nanotek. The technical specifications of the glass fiber, B₄C, and Gr powders used in the experiments are provided in Table 2.

2.2 Production of Composite

ARC 152 laminating epoxy resin and hardener were used in the production of composite materials. The epoxy resin material was supplied by Arc Marina Company. Following the recommendations of the company, 25 g of hardener was added to 100 g of resin. The amounts of resin and reinforcing elements to be used in the composite plates were measured using a Radwag precision scale. A mixture was prepared by adding B₄C and Gr separately in weight ratios of 5%, 10%, and 15% to the resin for use in composite plates. Composite plates were produced in composite laboratory using the hand lay-up method. Initially, the fibers were cut into dimensions of 30 cm × 30 cm to form the plates. Subsequently, the resin mixture was prepared. One of the cut fibers was placed on a flat surface, and the resin and filler mixture was applied



Table 2 Properties of glass fiber, B₄C and Gr

	Glass Fiber		B ₄ C	Gr
Areal weight	220 gr/m ²	Powder Size	30 μ	30 μ
Elongation at break	2.50%	Purity	96%	99.9%
Tensile strength	1300 MPa	Hardness	44 GPa	0.32 GPa
Elasticity modulus	65 GPa	Density	2.52 g/cm ³	2.09 – 2.23 g/cm ³

to the fabrics using a roller brush. A new fabric layer was placed on top of the first layer with resin, and this process was repeated. This process was repeated for a total of 13 layers. To prevent the fibers from sticking to the flat surface, the surface was covered with a transparent film. After the process was completed, another transparent film was placed on top of the fibers, and weight was placed on it. Unfilled composites were produced initially, followed by the production of composite plates filled with B₄C and Gr at ratios of 5%, 10%, and 15%. The prepared composite plates were cut according to standards on a circular saw machine for tensile, flexural, wear, and hole-drilling tests.

2.3 Tensile and Flexural Test

The specimens used in tensile tests were cut according to ASTM D638, and flexural tests were conducted according to ASTM D790 standards. The thickness of the specimens was 4 mm. A Shimadzu brand testing machine was used for both tensile and flexural tests. Throughout the experiment, data were transferred to the computer to determine the tensile strength and percentage elongation values of the specimens. Three tests were conducted for each parameter in both tensile and flexural tests, and the mean of the obtained results was taken. The experiments were conducted at a constant tensile speed of 1 mm/min. The flexural stress equation is given in Eq. 1.

$$\sigma_f = \frac{3PL}{2bd^2} \text{ (MPa)} \quad (1)$$

Here; σ_f : Flexural stress (MPa), P: Maximum load (N), L: Span between the two supports (mm), b: Width of the specimen (mm), and d: Thickness of the specimen (mm). The flexural strengths of the specimens were calculated using the formula given in Eq. 1.

2.4 Wear Test

Wear tests for filled composites necessitate the exploration of all combinations of experiments (varying load, sliding speed, filler ratio). Due to the significant costs in terms of both money and time associated with testing all these combinations, the Taguchi experimental design has been employed. The purpose of using Taguchi experimental design in this

study is to determine the relationships between all parameters with fewer experiments, covering all parameters in wear tests. Accordingly, the input parameters and levels for wear tests are provided in Table 3.

Taguchi method was employed with a three-factor mixed-level design to determine the impact of filler material, filler ratio, load, and sliding distance on wear. L36 (2¹–3³) design was selected as the mixed design in Taguchi method. Factors and levels were defined according to Taguchi method to create experimental combinations for filler material, filler ratio, force, and sliding distance. Graphs obtained from Taguchi design analysis program for wear tests were interpreted based on Signal-to-Noise (S/N) ratio graphs. Wear tests were conducted using a Turkeyus-brand pin-on-disk wear device, and the samples used in the experiments were of dimensions 40 mm × 40 mm. They were abraded by means of a steel ball with a diameter of 6 mm at a rotation speed of 300 rpm. Mass loss, wear rate, and specific wear rate were determinant factors in wear; and in this study, wear was calculated based on the wear rate. The equation used for the wear rate is given in Eq. 2.

$$\text{Wear Rate} = \frac{\Delta V}{S} \text{ (mm}^3/\text{m)} \quad (2)$$

Here; ΔV : Wear volume (mm³), S: Sliding distance (m).

Wear resistance can be defined as the material's resistance to mass loss or wear volume. Wear volume can be measured by either track width or track depth. In the wear tests conducted in this study, wear volume was calculated taking into account the track width formed on the material surface. The equation used to calculate the wear rate according to ASTM G99 standards is provided in Eq. 3.

$$WR = 2\pi * R [r^2 * \sin^{-1}(a/2*r) - (a/4) * (4 * r^2 - a^2)^{1/2}] \quad (3)$$

Here; WR represents the wear rate, R is the wear track radius, r denotes the ball radius, and a signifies the track width.

Table 3 Input parameters and levels for wear tests

Levels	Reinforcement fiber	Filler	Filler ratio (%)	Sliding distance (m)	Load (N)
1	Glass	Gr	5	250	5
2		B ₄ C	10	500	10
3			15	750	15

Table 4 Cutting parameters used for drilling

Spindle speed, N (rpm)	Feed rate, f (mm/rev)	Cutting speed, Vc (m/min)
500	0.025	6.25
1000	0.05	12.5
2000	0.1	25
4000	0.2	50

2.5 Drilling Experiment Equipment and Cutting Tools

Drilling experiments were conducted under dry cutting conditions on a Brother brand Speedio S500X1 CNC vertical machining center. The machining parameters used in the hole drilling experiments are presented in Table 4.

The drilling experiments on composite workpieces were performed in accordance with the parameters specified in Table 4. The geometric and coating characteristics of the drill and the drill bit used for drilling composite materials under dry cutting conditions are provided in Table 5.

The samples, measuring 25 mm × 130 mm, had a thickness of 4 mm, and the hole drilling process was applied throughout their length. For the hole drilling experiments, specially manufactured carbide drills with AlTiN coating, obtained from the Karcan cutting Tool Company, were used for drilling composite materials.

2.6 Delamination Factor

Delamination damage in composite materials is a crucial aspect concerning the structural integrity of the material. Delamination can be briefly described as the separation of layers in composite materials, and it is particularly critical in hole-drilling operations. Delamination is a commonly encountered damage type in laminated composites because the strength between layers is often low. Therefore, it frequently appears as a damage type in hole-drilling operations. Delamination in composite materials can lead to negative consequences such as loss of material life and stiffness. Hence, it is an important area of study. Delamination values at the exit of the hole were calculated as a result of hole-drilling operations conducted at four different cutting speeds and feed rates. Equation 4 was utilized to determine

the delamination factor in hole-drilling operations.

$$F_d = \frac{D_{max}}{D_o} \quad (4)$$

Delamination factor (F_d), as given in Eq. 4, is expressed as the ratio between the hole diameter (D_o) and the maximum damage radius around the hole (D_{max}). The experimental setup for machining experiments, including measurements of tensile strength, flexural strength, wear, friction coefficient, feed force, vibration, SEM, and delamination factor, is illustrated in Fig. 1.

3 Experimental Results and Discussion

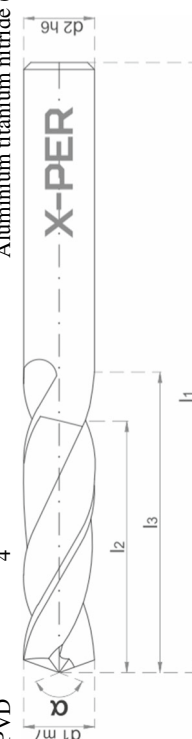
3.1 Tensile Test Results

Tensile strength and percentage elongation values of filled GFRC are shown in Table 6. The graphs of tensile stress and percentage elongation values for composite materials in Table 6 are provided in Fig. 2 and Fig. 3. When the tensile stress values in Fig. 2 and Fig. 3 are examined, it is evident that the addition of both Gr and B₄C filler particles to GFRC results in a decrease in tensile strength. Additionally, an increase in the filler ratio in GFRC is determined reduction in the tensile strength of the composite materials.

GFRCs' tensile strength values decreased after the addition of filler particles, and this is believed to be due to the increased filler content leading to agglomeration and non-uniform distribution within the structure, resulting in a weak filler-matrix-fiber bond. The results obtained from tensile tests are consistent with previous studies [44]. Baptista et al. stated that the addition of up to 10% Gr by weight to the fiber-reinforced composite reduced the tensile strength. The authors attributed the decrease in the tensile strength of the Gr reinforced composite to the formation of macro and micro voids in the matrix and the separation of Gr agglomerations [45]. Additionally, Yasmin and Daniel reported that mechanical properties improved up to 2.5% Gr reinforcement rate, and when this rate was exceeded, tensile strength tended to decrease. The increase in tensile strength was attributed to the good adhesion between the matrix and the reinforcement and the homogeneous distribution of the reinforcement within the matrix. However, they stated that the reason for the decrease in tensile strength when the 2.5% Gr reinforcement rate is

Table 5 Geometric and coating properties of the cutting tool

d1m7	d2h6	Point angle α	Helix angle	Clearance angle	l1	l2	l3
4	6	118°	30°	11°	66	22	24
Coating type	Number of coating layers	Coating composition	Coating thickness				
PVD	4	Aluminium titanium nitride (AlTiN)	1.78 μm				



exceeded is due to the brittleness of the matrix and the accumulation of Gr in certain areas within the composite [46]. When the changes in elongation values in Fig. 2, 3 are examined, it is understood that the addition of Gr and B₄C fillers to GFRCs increases the composite's percentage elongation values. Shivamurthy et al. found that the tensile strength of GFRC with Gr filler increased up to a 6% filler ratio, but decreased at a 9% Gr filler ratio. They attributed the increase in tensile strength up to a certain filler ratio to the strong bonding between the filler and the matrix. Additionally, they observed an increase in longitudinal elongation at 3% and 6% filler ratios, but a decrease at a 9% filler ratio [47]. The strength of composites filled with 5% and 15% Gr decreased by 18% and 52%, respectively, compared to the unfilled composite. For composites with 5% and 15% B₄C, the strength decreased by 39% and 47%, respectively.

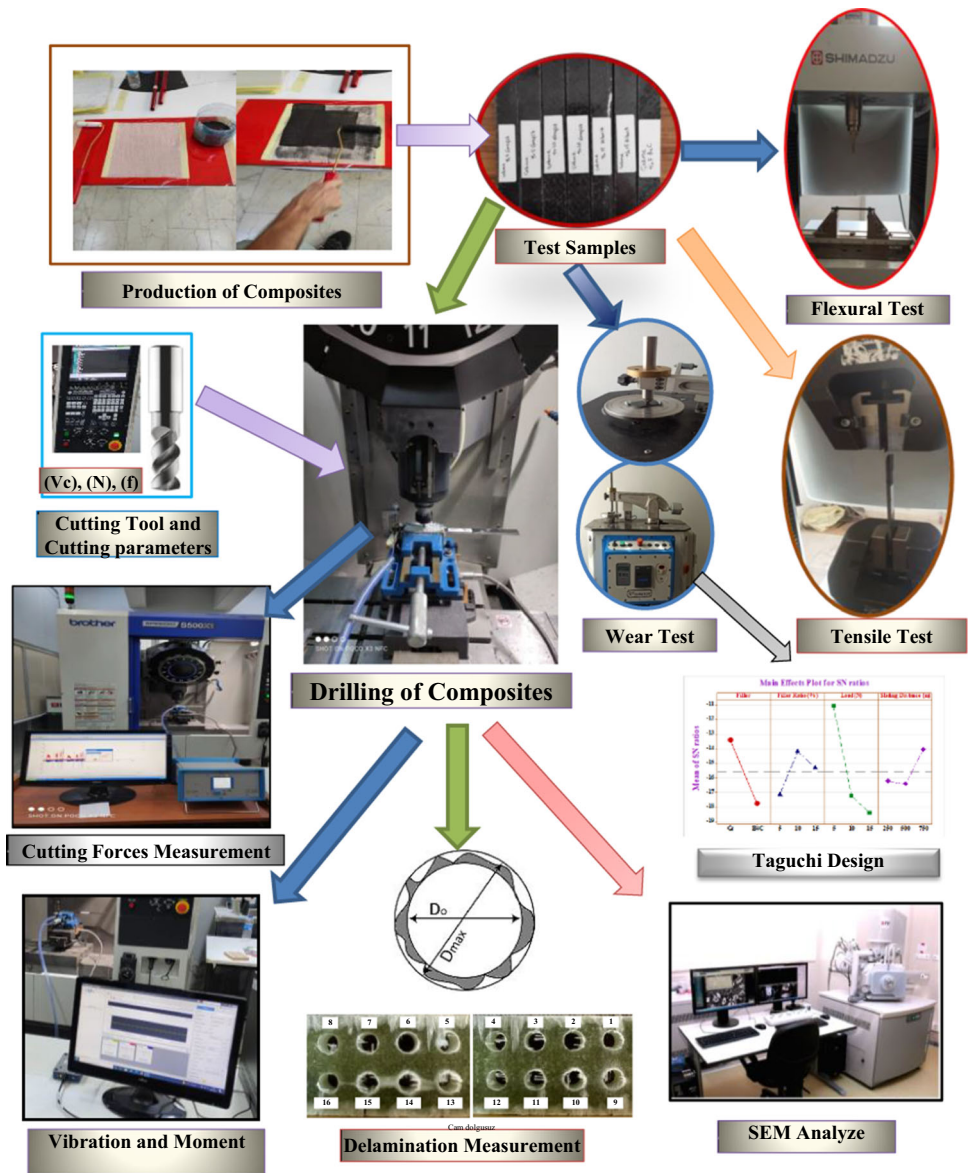
When the tensile strength in Figs. 2, 3 are examined, it is observed that B₄C filler reduces tensile strength more than Gr filler. This is thought to be due to the weaker bond formed between B₄C filler and the matrix, and its geometric shape having sharper corners, which create stress concentration points during tension, and cause notching effects, thereby reduce the strength of the composite material.

3.2 Flexural Test Results

The flexural test results of unfilled and filled composite materials are presented in Table 7, and the flexural test graphs are shown in Figs. 4, 5. Upon examination of the graphs in Figs. 4, 5, it is observed that the flexural strengths of both B₄C and Gr-filled composites in GFRCs increased up to a 10% filler ratio. However, when the filler ratio was increased to 15%, the flexural strength for both types of fillers fell below even the flexural strength of the unfilled composite. The highest flexural strength in Gr and B₄C-filled composites was obtained at a 10% filler ratio, reaching 368 MPa and 384 MPa, respectively. Studies on B₄C-filled composites have also indicated an increase in flexural strength up to a certain filler ratio, followed by a decrease beyond a critical filler ratio [44, 48]. The reason for this is explained that the filler ratio exceeding a certain limit, prevents sufficient wetting by the matrix, and results in the formation of voids due to agglomeration. It is well-known that the interfacial bonds between the filler material and the matrix or proper wetting of filler particles by the matrix, leading to homogeneous filler distribution, have a significant impact on the mechanical properties of composites. In another study, the increase in flexural strength in Gr reinforced composite is attributed to the increase in the load carrying capacity of the composite due to the high bonding and cohesion between the matrix and the particle [45–49]. Bhatia et al. [50] explained in their study on B₄C-filled epoxy composites that beyond a certain ratio, the flexural strength



Fig. 1 Schematic representation of the experimental setup



showed a decreasing trend, attributing this to the agglomeration of particles with high surface energy and the matrix material embrittlement because of hard ceramic particles.

Upon examination of the graphs in Figs. 4, 5, it is evident that in GFRCs, B₄C filler increased flexural strength more than Gr filler. The greater hardness of B₄C compared to Gr contributed to the higher flexural strength of B₄C-filled composites. Since B₄C has higher hardness and a stronger cross-linking with epoxy and glass fiber, it has achieved higher flexural strength compared to Gr reinforced composite, as it further increases the load transfer ability of B₄C reinforced composite. However, the addition of higher ratios created a weaker bond between the matrix and the particle, resulting in a decrease in flexural strength. The results are consistent with previous studies [12, 50].

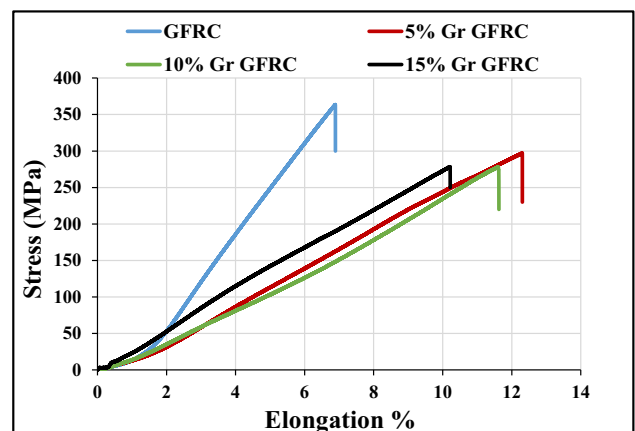
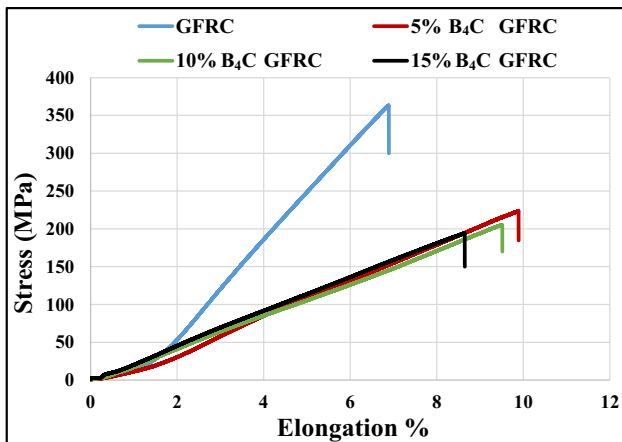


Fig. 2 Stress–strain graph of unfilled and Gr-filled GFRC

Table 6 Tensile test results

Fiber type	Samples	Tensile stress (MPa)	Elongation % (mm)
Glass	Unfilled	363	6.89
Glass	5% Gr	297	12.3
Glass	10% Gr	278	11.62
Glass	15% Gr	173	7.85
Glass	5% B ₄ C	223	9.89
Glass	10% B ₄ C	205	9.51
Glass	15% B ₄ C	194	8.64

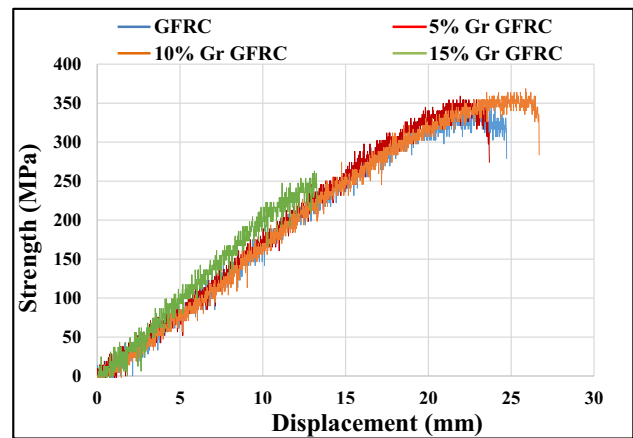
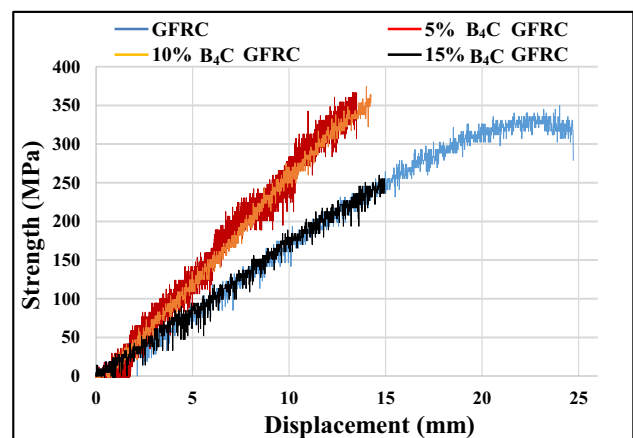
**Fig. 3** Stress-strain graph of unfilled and B₄C-filled GFRC**Table 7** Flexural test results

Fiber type	Samples	Flexural (MPa)
Glass	Unfilled	349
Glass	5% Gr	358
Glass	10% Gr	368
Glass	15% Gr	259
Glass	5% B ₄ C	365
Glass	10% B ₄ C	384
Glass	15% B ₄ C	262

3.3 Wear Test Results

The experimental combinations and results of the wear rate of filled composites, generated by Taguchi mixed design, are provided in Table 8. The S/N ratios for wear rates based on filler type, filler ratios, force, and sliding distance in Table 8 are illustrated in Fig. 6.

In Fig. 6, when B₄C and Gr-filled composites are compared, it is evident that B₄C filler increases the wear rate more than Gr filler. When reviewing the literature, it is known

**Fig. 4** Flexural-displacement graph of unfilled and Gr-filled GFRC**Fig. 5** Flexural-displacement graph of unfilled and B₄C-filled GFRC

that Gr enhances wear resistance due to its solid lubricating properties [26, 51]. Regarding the effect of filler ratios, it is observed that composites with 5% filler experience more wear compared to those with 10% and 15% filler ratios. When the filler ratio is increased from 10 to 15%, there is a slight decrease in wear resistance. It can be suggested that beyond a certain ratio, abrasive particles within the composite exit the matrix, causing an abrasive effect between the composite and the steel ball during wear [19]. Analyzing the influence of applied force on the wear rate in Fig. 6, it is found that increasing the force from 5 to 10N significantly increases the wear rate. However, when the force is increased from 10 to 15N, the rate of increase in wear becomes lower. Similar results have been encountered in studies in the literature [52, 53]. Examining the effect of sliding distance on wear, it is noticed that the wear rate initially increases up to a sliding distance of 500 m, and then decreases when the sliding distance is increased to 750 m. Suresha et al., in their study, observed a decrease in wear rate with increasing sliding distances, which is consistent with the findings here [26]. In

Table 8 Wear test combinations generated by Taguchi mixed design for filler type, filler ratio, forces, and sliding distance

Exp. No	Material	Filler type	Filler ratio (%)	Forces (N)	Sliding distance (m)	Friction coefficient	Friction coefficient S/N	Wear rate	Wear rate S/N
1	Glass	Gr	5	5	250	0.758695	2.39865	4.5510	-13.1621
2	Glass	Gr	10	10	500	0.522985	5.63021	7.2057	-17.1536
3	Glass	Gr	15	15	750	0.410000	7.74432	7.2236	-17.1751
4	Glass	Gr	5	5	250	0.758695	2.39865	4.5510	-13.1621
5	Glass	Gr	10	10	500	0.522985	5.63021	7.2057	-17.1536
6	Glass	Gr	15	15	750	0.410000	7.74432	7.2236	-17.1751
7	Glass	Gr	5	5	500	0.915565	1.98649	3.7778	-11.5447
8	Glass	Gr	10	10	750	0.489150	6.21117	8.3722	-18.4568
9	Glass	Gr	15	15	250	0.320000	8.40433	9.0133	-19.0977
10	Glass	B ₄ C	5	5	750	0.738546	0.55088	8.8085	-18.8980
11	Glass	B ₄ C	10	10	250	0.655047	3.67456	13.4139	-22.5511
12	Glass	B ₄ C	15	15	500	0.378976	8.42777	20.0989	-26.0634
13	Glass	B ₄ C	5	10	750	0.496672	6.07860	12.6309	-22.0287
14	Glass	B ₄ C	10	15	250	0.335832	9.47756	16.2165	-24.1992
15	Glass	B ₄ C	15	5	500	0.647041	3.78137	9.1930	-19.2692
16	Glass	B ₄ C	5	10	750	0.496672	6.07860	12.6309	-22.0287
17	Glass	B ₄ C	10	15	250	0.335832	9.47756	16.2165	-24.1992
18	Glass	B ₄ C	15	5	500	0.647041	3.78137	9.1930	-19.2692
19	Glass	Gr	5	10	250	0.668332	3.50016	8.3324	-18.4154
20	Glass	Gr	10	15	500	0.542240	5.31616	5.8437	-15.3338
21	Glass	Gr	15	5	750	0.588256	4.60867	1.6550	-4.3760
22	Glass	Gr	5	10	500	0.599968	6.02115	5.8437	-15.3338
23	Glass	Gr	10	15	750	0.353759	9.02585	3.0400	-9.6574
24	Glass	Gr	15	5	250	0.619504	4.15911	2.7745	-8.8636
25	Glass	Gr	5	15	500	0.499968	6.02115	7.2057	-17.1536
26	Glass	Gr	10	5	750	0.542229	5.31634	1.7763	-4.9903
27	Glass	Gr	15	10	250	0.427037	7.39069	3.2315	-10.1882
28	Glass	B ₄ C	5	15	500	0.607565	4.61888	8.7690	-18.8590
29	Glass	B ₄ C	10	5	750	0.708167	2.99729	3.8958	-11.8120
30	Glass	B ₄ C	15	10	250	0.717673	2.88147	6.6875	-16.5052
31	Glass	B ₄ C	5	15	750	0.577362	4.77104	7.0325	-16.9423
32	Glass	B ₄ C	10	5	250	0.930967	0.06017	3.0745	-9.7555
33	Glass	B ₄ C	15	10	500	0.767687	2.29631	5.8437	-15.3338
34	Glass	B ₄ C	5	15	250	0.564896	4.96062	9.3357	-19.4030
35	Glass	B ₄ C	10	5	500	0.951588	0.43102	2.5542	-8.1453
36	Glass	B ₄ C	15	10	750	0.786710	2.08370	6.5399	-16.3114

Fig. 6, when the graphs of the wear rate are examined, it is determined that forces have the greatest impact on the wear rate depending on S/N ratios. The sliding distance appears to have the least impact on the wear rate. Table 8 provides the graphical representation of S/N ratios for friction coefficient values based on filler type, filler ratios, load, and sliding distance, as shown in Fig. 7. When the S/N ratio graph in Fig. 7

is examined and filler types are compared, it is observed that the friction coefficients of Gr-filled glass fiber composites are lower than those of B₄C-filled glass fiber composites. This situation is attributed to B₄C particles exiting the matrix during wear, getting trapped between the pin and the material, leading to an increase in the friction coefficient.

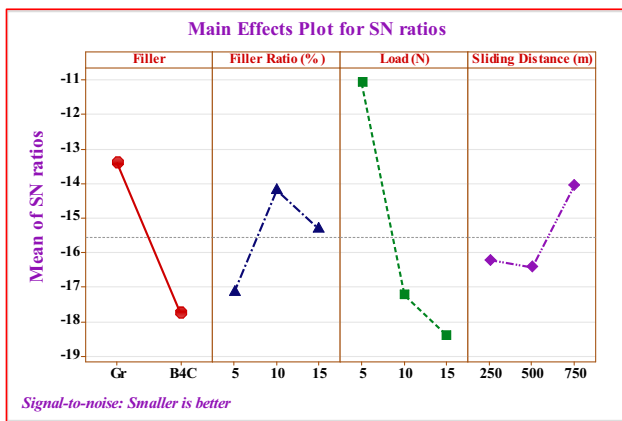


Fig. 6 Wear rate graph (mm^3/m) depending on Filler, Filler Ratio, Load and Sliding Distances

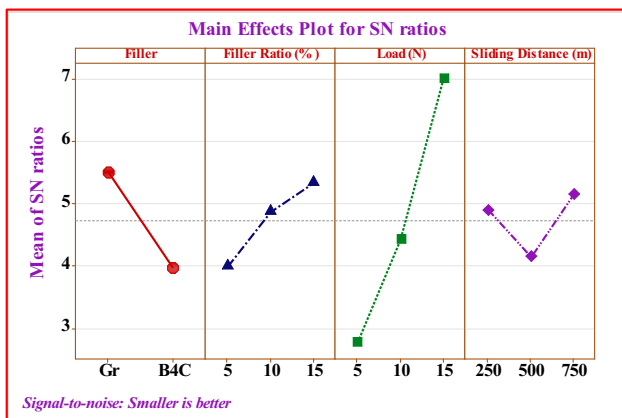


Fig. 7 Friction Coefficient Graph depending on Filler, Filler Ratio, Load and Sliding Distances

When the effect of the filler type is examined, filler ratios, force, and sliding distance on the friction coefficient ratios presented in Table 8, graphical representation in Fig. 7 is provided. Upon analyzing S/N ratios in Fig. 7, it is evident that glass fiber-reinforced composites with Gr reinforcement exhibit lower friction coefficients compared to those with B₄C reinforcement. This may be attributed to B₄C particles exiting the matrix during abrasion, getting trapped between the pin and the material, leading to an increase in the friction coefficient. Regarding the influence of the filler ratio, it is observed that the friction coefficients of both Gr and B₄C-filled composites decrease with increasing filler ratios. This reduction is attributed to the lubricating property of Gr particles and the high hardness of B₄C particles, causing the friction coefficients of Gr and B₄C-filled composites to decrease with increasing filler ratios. In Fig. 7, the effect of the load is examined, and it is observed that the friction coefficient decreases with an increase in load for both Gr and B₄C. At higher loads, Gr particles separating from the

sample surface create a thin tribo-surface between the sample and the sliding surface, acting as a lubricant and thereby assisting in reducing the friction coefficient. This observation aligns with the findings of Shivamurthy et al.'s study [47]. In B₄C-reinforced composites, the reduction in wear rate and friction coefficient can be attributed to two main reasons. Firstly, the increased hardness of the matrix due to B₄C enhances wear resistance. Secondly, during wear, B₄C ceramic particles embedded in the epoxy form a barrier between the composite and the counterface, thereby reducing wear [54]. Similar studies also confirm this situation [55, 56]. Analyzing the effect of the sliding distance, it is observed that with an increasing sliding distance, the friction coefficient initially increases and then tends to decrease again. This phenomenon can be explained by the abrasive steel ball initially abrading the soft matrix material, followed by the revealed Gr and B₄C reinforcements reducing direct contact between the abrasive pin and the sample, resulting in a decrease in the friction coefficient. Upon a closer inspection of the graph in Fig. 7, it is determined that forces have the greatest impact on the friction coefficient, while the sliding distance has the least effect on it, as indicated by S/N ratios.

3.4 SEM Morphology

3.4.1 SEM Morphology of Worn Surfaces

SEM images of worn surfaces for Gr and B₄C-filled composites under different parameters (reinforcement ratio, load, and sliding distance) are presented in Fig. 8. When Fig. 8a, b are examined for Gr-filled composites, it is observed that increasing Gr filler ratio from 5 to 15% under the same load and sliding distance results in narrower wear scars and less exposure to abrasion. The lubricating property of Gr reinforcement in abrasion has made the material more resistant to wear with an increased reinforcement ratio. With higher Gr reinforcement, fewer pits, cracks, and matrix fractures are observed on the worn surface. Previous studies by Suresha et al. and Basavarajappa et al. noted that Gr filler enhances the tribological properties of composites [11, 57]. When SEM images in Fig. 8c, d are examined, it is seen that increasing the load under constant reinforcement ratio and sliding distance significantly widens the wear track. With increased load, wear pits become more pronounced, matrix fractures increase, and the number of voids in the matrix rises, evolving from a smoother surface to a more damaged one. In Fig. 8e, f, SEM images indicate that increasing the sliding distance under constant reinforcement ratio and load intensifies abrasion. As the distance increases, fiber abrasion and tearing lead to the rupture of some fibers in long fiber bundles, causing more deformation in the matrix layer, and a porous and cavity-like structure become more pronounced.

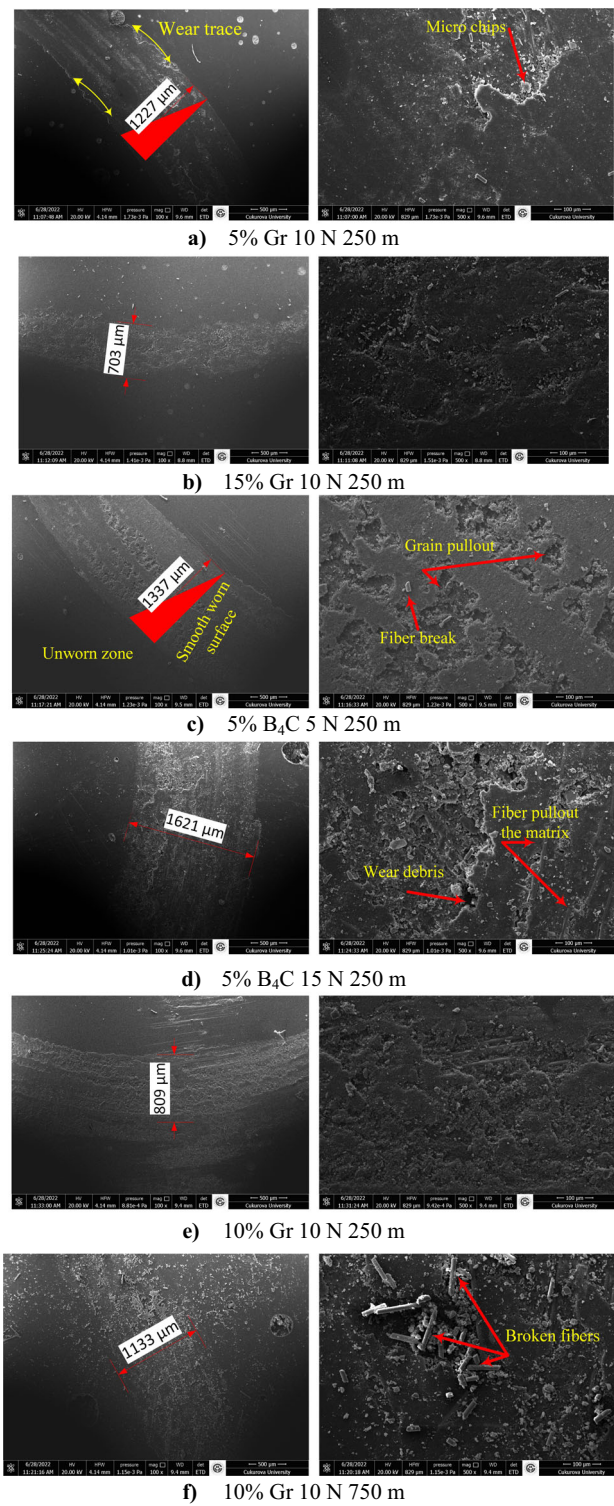


Fig. 8 SEM images of worn surfaces under the influence of reinforcement, load, and sliding distance

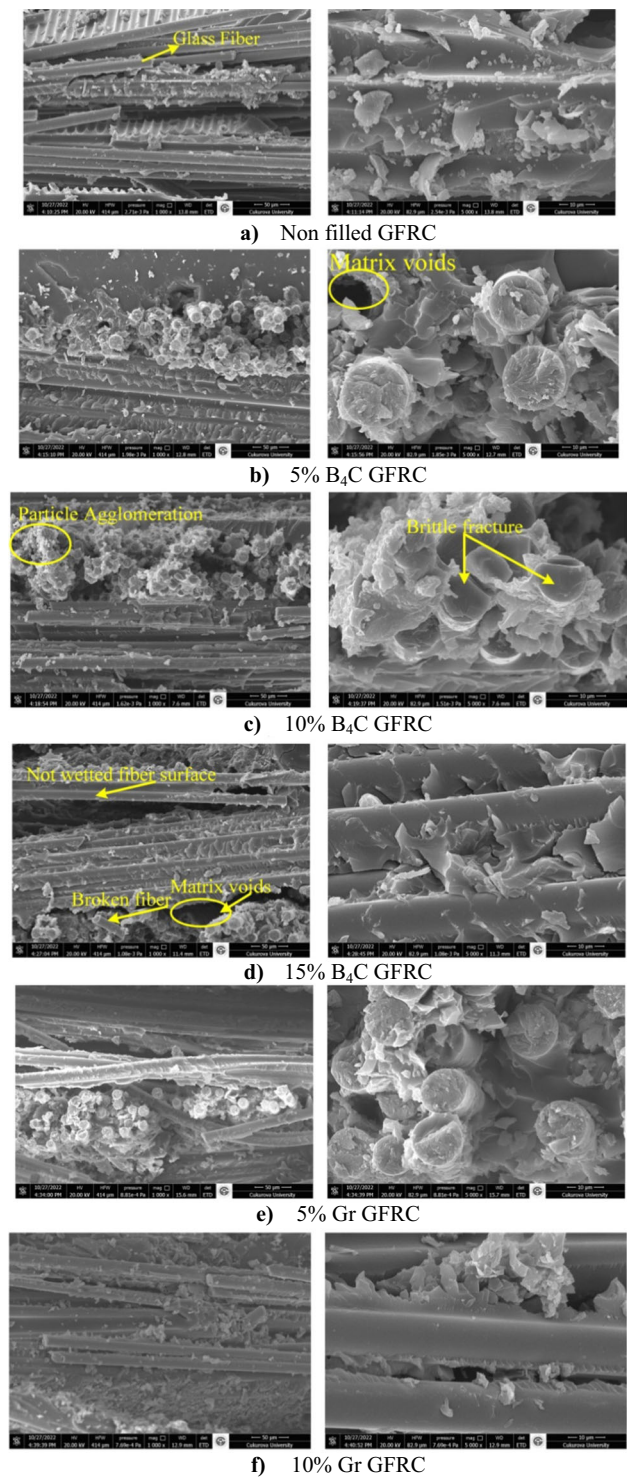


Fig. 9 SEM images of fractured surfaces after tensile testing under the influence of reinforcement, load, and sliding distance

3.4.2 SEM Morphology of Fractured Surfaces

SEM images of fracture surfaces of filled and unfilled GFRC are shown in Fig. 9. When the fracture section morphologies of GFRC are examined, it is observed in Fig. 9a that the adhesion between the matrix and the fibers is better in unfilled composites. With the addition of fillers and an increase in filler ratio, the adhesion between matrix-filler and matrix-fiber decreases progressively. The matrix fails to wet both the fibers and filler particles, resulting in an increase in voids in the fracture section and a subsequent decrease in load-carrying capacity (Fig. 9b–d).

The most crucial parameter in filler addition is the homogeneous distribution and dispersion of the filler within the matrix, leading to an increase in the load-carrying capacity of the composite. As seen in Fig. 9c–f, filler particles accumulate at certain points on the fiber. In their study, Shivamurthy et al. found that the addition of 3% Gr filler to GFRC increased tensile strength. However, when this ratio was exceeded, tensile strength started to decrease, as observed in both SEM images and tensile test results [47].

3.5 Evaluation of the Thrust Forces

Through-hole drilling was carried out on GFRC samples at 5%, 10% and 15% Gr and B₄C filler rates at 4 different feed rates and 4 different cutting speeds. The thrust forces obtained during drilling of unfilled, Gr and B₄C filled, GFRCs at different cutting parameters are given in Figs. 10. When the thrust force graphs in Fig. 10 are examined, it is seen that the thrust forces decrease when the cutting speed increases. This result is parallel to the literature [58]. When the cutting speed increases, the temperature in the cutting zone will increase. This will contribute to the softening of the material and help reduce thrust forces by making drilling easier. When the feed force graphs obtained in drilling unfilled, Gr and B₄C filled, GFRCs obtained under different cutting parameters were examined, it was determined from the graphs in Fig. 10 that the thrust forces increased with the increase of the feed rate. This is similar to studies conducted in the literature [19, 59]. Increasing the feed rate increases the load on the drill by increasing the chip removal volume removed per unit time, and at the same time, increasing friction and chip jamming during feed causes the thrust forces to increase. When the graphs in Fig. 10 are examined, it is observed that the lowest thrust force is obtained at the cutting parameters $V_4 = 50$ m/min and $f_1 = 0.025$ mm/rev, while the highest thrust force value is obtained at $V_1 = 6.25$ m/min and $f_4 = 0.2$ mm/rev. The thrust force change graphs obtained depending on different cutting and feed speeds of Gr and B₄C filled GFRCs are given in Fig. 10. When the graphs in Fig. 10 are examined, it is seen that the thrust forces obtained in drilling B₄C filled GFRCs are higher compared to Gr filled

GFRCs. The reason for this is that the B₄C ceramic filler material has a very high hardness, causing the drill to become more difficult during drilling, resulting in higher feed forces. The fact that the Gr filler is softer compared to the B₄C filled material ensures that the feed forces are lower during drilling. In addition, the lubricating properties of Gr also contributed to the low forces [26, 51].

The trust force change graphs obtained depending on different cutting speeds and feed rates of unfilled and B₄C filled GFRC are given in Fig. 10. When the graphs in Fig. 10 are examined, it is determined that B₄C filling material and filling ratio increase the trust forces at significant rates. Increasing the B₄C filling ratio increased the hardness of the composite material, causing the trust forces to increase remarkably.

3.6 Evaluation of Vibration and Moments

The highest trust forces were obtained for the vibration and moment values measured during the drilling of glass fiber reinforced samples at 5%, 10% and 15% B₄C and Gr filler ratios ($V_1 = 6.25$ m/min and $f_4 = 0.2$ mm/rev). And the measurements at the cutting parameters where the lowest trust forces were obtained ($V_4 = 50$ m/min and $f_1 = 0.025$ mm/rev) were taken as reference. Because the measured vibration and moment values were very close to each other, and they were evaluated by taking into account the measurements of the cutting parameters where the highest and lowest trust forces were obtained. Vibration and moment values obtained depending on different cutting speeds and feed rates of glass fiber reinforced epoxy composites at 5%, 10% and 15% Gr and B₄C filler ratios are given in Table 9. When the vibration and moment values in Table 9 are examined, it is seen that there is no significant difference between the vibration and moment values of glass fiber reinforced epoxy composites, depending on the changing machining parameters. When both vibration and moment values of GFRCs depending on the filling type are examined in Table 8, it is determined that both vibration and moment values of B₄C composite materials were higher than both vibration and moment values of Gr composite materials. This can be explained by the fact that both vibration and moment values occurring during drilling are higher because GFRCs with B₄C filler ratio are harder than GFRCs with Gr filler ratio.

3.7 Evaluation of Delamination Measurements

Delamination measurements were carried out after the through-hole drilling process of GFRCs at 5%, 10% and 15% Gr and B₄C filler ratios at 4 different feed rates and 4 different cutting speeds. Delamination were measured from the hole exit. Delamination values obtained during drilling of unfilled, Gr and B₄C filled GFRCs at different cutting parameters are given in Fig. 11. When the delamination graphs in Fig. 11

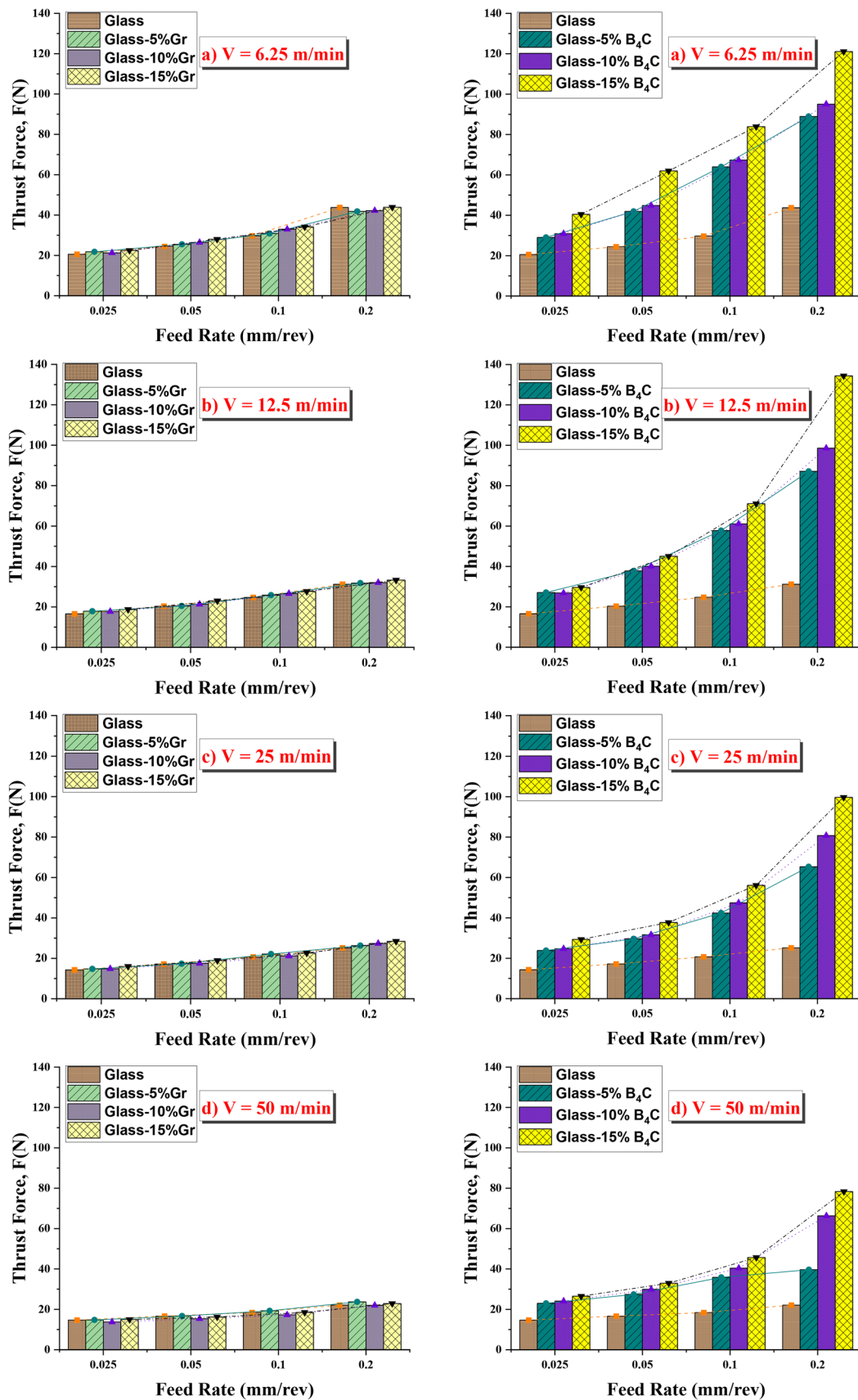


Fig. 10 Change of thrust forces obtained depending on the feed rate of unfilled, Gr and B_4C -filled GFRCs at different cutting speeds

Table 9 Vibration and moment values of GFRCs

Cutting parameters	Material type	Moment	Vibration
$V_1 = 6.25$ m/min and $f_4 = 0.2$ mm/rev	Unfilled	1.163	0.085459
$V_4 = 50$ m/min and $f_1 = 0.025$ mm/rev		0.22	0.085210
$V_1 = 6.25$ m/min and $f_4 = 0.2$ mm/rev	Glass 5% Gr	1.18	0.085275
$V_4 = 50$ m/min and $f_1 = 0.025$ mm/rev		0.24	0.085130
$V_1 = 6.25$ m/min and $f_4 = 0.2$ mm/rev	Glass 10% Gr	1.28	0.085311
$V_4 = 50$ m/min and $f_1 = 0.025$ mm/rev		0.29	0.085180
$V_1 = 6.25$ m/min and $f_4 = 0.2$ mm/rev	Glass 15% Gr	1.43	0.086321
$V_4 = 50$ m/min and $f_1 = 0.025$ mm/rev		0.41	0.086105
$V_1 = 6.25$ m/min and $f_4 = 0.2$ mm/rev	Glass 5% B ₄ C	2.69	0.087051
$V_4 = 50$ m/min and $f_1 = 0.025$ mm/rev		0.89	0.864450
$V_1 = 6.25$ m/min and $f_4 = 0.2$ mm/rev	Glass 10% B ₄ C	2.96	0.087190
$V_4 = 50$ m/min and $f_1 = 0.025$ mm/rev		0.37	0.086589
$V_1 = 6.25$ m/min and $f_4 = 0.2$ mm/rev	Glass 15% B ₄ C	3.42	0.087349
$V_4 = 50$ m/min and $f_1 = 0.025$ mm/rev		0.65	0.086788

are examined, it is seen that delamination values increase when the cutting speed increases. The findings are consistent with the literature [60, 61]. Increasing temperature due to friction at high cutting speeds reduces the matrix toughness, causing the hole diameter to increase and as a result, delamination values also increase. When the delamination graphs obtained in the drilling of unfilled, Gr and B₄C filled GFRCs obtained at different cutting parameters are examined, it is determined from the graphs in Fig. 11 that the delamination values decreased with the increase of the feed rate. This is similar to studies conducted in the literature [62, 63]. Increasing the drilling time at low feed rates causes high friction between the cutting tool and the composite material, which generates more heat in the drilling area. In this case, it is thought to have a negative effect on delamination due

to the increase in thermal damage at the hole exit. Therefore, increasing the feed rate causes the delamination values to decrease. When the graphs in Fig. 11 are examined, in GFRCs, the lowest delamination values are obtained at the cutting parameters $V_1 = 6.25$ m/min and $f_4 = 0.2$ mm/rev, while the highest delamination values are obtained at $V_4 = 50$ m/min and $f_1 = 0.025$ mm/rev. The change graphs of delamination values obtained depending on different cutting and feed rates for unfilled and Gr-filled GFRCs are given in Fig. 11. The reason for this is due to the lubricating properties of Gr contained in Gr reinforced composites. The change graphs of delamination values obtained depending on different cutting and feed rates for unfilled and B₄C filled GFRCs are given in Fig. 11. When the graphs in Fig. 11 are examined, it is observed that delamination values in 5%, 10% and 15% B₄C filled GFRCs are lower than unfilled glass. It was determined that B₄C filling material and filling ratio reduced the delamination values (Fig. 11). Increasing the filling material and filling ratio helped to reduce the delamination values by increasing the hardness of the produced composite. When Gr and B₄C filled GFRCs are compared, it is determined that the delamination values of B₄C filled GFRCs are generally higher than the delamination values of Gr filled GFRCs. The fact that B₄C is harder than Gr caused higher delamination values.

4 Conclusions

In this study, B₄C and Gr filled GFRCs were produced. The mechanical, tribological and drilling performances of the produced composite samples were investigated. The results obtained are listed below.

- The addition of 15% Gr to unfilled GFRC reduced the tensile strength of the composite from 363 to 173 MPa. Both B₄C and Gr fillers reduced the tensile strength of GFRCs. The tensile strength was obtained as 194 MPa at 15% B₄C filler ratio. The flexural strength increased in both Gr and B₄C filler types up to 10% filler ratio in glass fiber reinforced composites. At 15% filler rates, flexural strength started to decrease for both filler types.
- Gr filler improved the wear resistance more than B₄C filler. Increasing the filler rate by 10% reduced the wear rate, while 15% filler rate increased it slightly. It was observed that the wear rate increased with increasing load. Increasing both the filler ratio and load in GFRCs reduced the friction coefficient.
- SEM images revealed that with increasing filler rate, the wear marks narrowed and the composite material surface wore less. Matrix debris and fiber cracks increased with increasing loads. Surface deformation, cavities and cracks were lesser at low sliding distances.

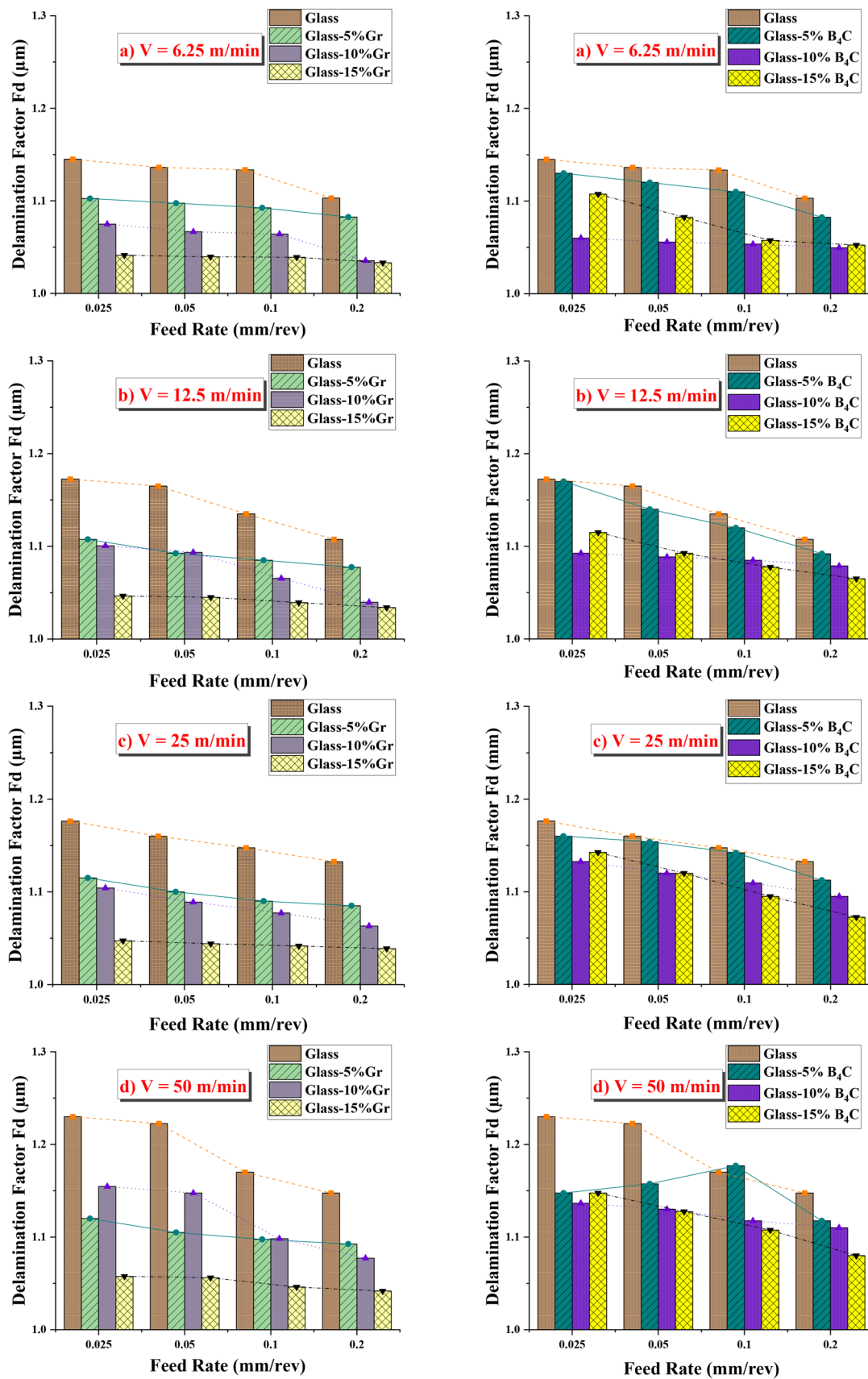


Fig. 11 Change of delamination values obtained depending on the feed rate of unfilled, Gr and B_4C -filled GFRCs at different cutting speeds

- GFRCs, feed forces increased depending on the increase in feed speed, and decreased due to the increase in cutting speed. While Gr filling did not provide a significant increase in the thrust forces, B₄C filler provided a significant increase.
- Delamination values in GFRCs decreased with increasing feed rate and increased with increasing cutting speed. Delamination values decreased with increasing Gr filling in GFRCs. In B₄C filled GFRCs, the lowest delamination values were obtained at 10% B₄C filling ratio.
- There was no significant difference between the vibration and moment values of GFRCs, depending on the changing machining parameters. The vibration and moment values of B₄C filled GFRCs were higher than the values obtained in Gr filled GFRCs.
- The Taguchi experimental design used for wear experiments made a significant contribution in terms of both cost and time by determining the relationship between all parameters with a smaller number of experiments to cover all parameters. Depending on S/N ratios, it was determined that the forces had the greatest effect on the wear rate and friction coefficient, and the sliding distance had the least effect.

Acknowledgements The authors would like to thank Batman University BAP unit (Project numbered BTÜBAP-2021-YL-020) for providing all kinds of contributions and support in the realization of this experimental study.

Funding Open access funding provided by the Scientific and Technological Research Council of Türkiye (TÜBİTAK).

Declarations

Conflict of interest The authors declare that they have no conflict of interest.

Open Access This article is licensed under a Creative Commons Attribution 4.0 International License, which permits use, sharing, adaptation, distribution and reproduction in any medium or format, as long as you give appropriate credit to the original author(s) and the source, provide a link to the Creative Commons licence, and indicate if changes were made. The images or other third party material in this article are included in the article's Creative Commons licence, unless indicated otherwise in a credit line to the material. If material is not included in the article's Creative Commons licence and your intended use is not permitted by statutory regulation or exceeds the permitted use, you will need to obtain permission directly from the copyright holder. To view a copy of this licence, visit <http://creativecommons.org/licenses/by/4.0/>.

References

1. Asi, O.: An experimental study on the bearing strength behavior of Al₂O₃ particle filled glass fiber reinforced epoxy composites pinned joints. *Compos. Struct.* **92**(2), 354–363 (2010)
2. Kumar, S.; Singh, K.K.; Ramkumar, J.: Comparative study of the influence of graphene nanoplatelets filler on the mechanical and tribological behavior of glass fabric-reinforced epoxy composites. *Polym. Compos.* **41**(12), 5403–5417 (2020)
3. Du, Y.; Zhang, Z.; Wang, D.; Zhang, L.; Cui, J.; Chen, Y.; Jiang, N.: Enhanced tribological properties of aligned graphene-epoxy composites. *Friction* **10**(6), 854–865 (2022)
4. Reddy, M.K.; Kiran, Z.S.; Babu, V.S.; Ram, V.: Sliding wear characteristics of epoxy-glass composites reinforced with micro B₄C. In AIP Conference Proceedings (Vol. 2269, No. 1). AIP Publishing (2020) October.
5. Wang, Q.; Zhang, X.; Pei, X.: Study on the synergistic effect of carbon fiber and graphite and nanoparticle on the friction and wear behavior of polyimide composites. *Mater. Des.* **31**(8), 3761–3768 (2010)
6. Hulugappa, B.; Achutha, M.V.; Suresha, B.: Effect of fillers on mechanical properties and fracture toughness of glass fabric reinforced epoxy composites. *JMMCE* **4**(1), 1–14 (2016)
7. Suresha, B.; Ramesh, B.N.; Subbaya, K.M.; Kumar, B.R.; Chandramohan, G.: Influence of graphite filler on two-body abrasive wear behaviour of carbon fabric reinforced epoxy composites. *Mater. Des.* **31**(4), 1833–1841 (2010)
8. Durairaj, S.; Chandramohan, P.; Rajesh, R.: Evaluation of mechanical properties of B₄C filled glass-epoxy composites. *Int. J. Chemtech Res.* **8**, 1997–1981 (2015)
9. Patil, N.; Krishna, P.: Friction and wear study of graphite and bronze filled epoxy matrix composites. *Mater. Today: Proc.* **59**, 134–137 (2022)
10. Mohan, N.; Natarajan, S.; Kumares Babu, S.P.: Abrasive wear behaviour of hard powders filled glass fabric-epoxy hybrid composites. *Mater. Des.* **32**(3), 1704–1709 (2011)
11. Basavarajappa, S.; Ellangovan, S.; Arun, K.V.: Studies on dry sliding wear behaviour of graphite filled glass-epoxy composites. *Mater. Des.* **30**(7), 2670–2675 (2009)
12. Asi, O.: Mechanical properties of glass-fiber reinforced epoxy composites filled with Al₂O₃ particles. *J. Reinf. Plast. Compos.* **28**(23), 2861–2867 (2009)
13. Demir, M.E.; Cetkin, E.; Ergün, R.K.; Denizhan, O.: Tribological and mechanical properties of nanofilled glass fiber reinforced composites and analyzing the tribological behavior using artificial neural networks. *Polym. Compos.* **45**(5), 4233–4249 (2024)
14. Borrego, L.P.; Costa, J.D.M.; Ferreira, J.A.M.; Silva, H.: Fatigue behaviour of glass fibre reinforced epoxy composites enhanced with nanoparticles. *Compos. B Eng.* **62**, 65–72 (2014)
15. Fathy, A.; Shaker, A.; Hamid, M.A.; Megahed, A.A.: The effects of nano-silica/nano-alumina on fatigue behavior of glass fiber-reinforced epoxy composites. *J. Compos. Mater.* **51**(12), 1667–1679 (2017)
16. Raju, B.R.; Suresha, B.; Swamy, R.P.; Bharath, K.N.: The effect of silicon dioxide filler on the wear resistance of glass fabric reinforced epoxy composites. *Polym. Compos.* **18**, 20 (2012)
17. Sarkar, P.; Modak, N.; Sahoo, P.: Effect of aluminum filler on friction and wear characteristics of glass epoxy composites. *SILICON* **10**, 715–723 (2018)
18. Anjum, N.; Ajit Prasad, S.L.; Suresha, B.: Role of silicon dioxide filler on mechanical and dry sliding wear behaviour of glass-epoxy composites. *Advances in tribology*, (2013).
19. Raju, B.R.; Suresha, B.; Swamy, R.P.; Kanthraju, B.S.G.: Investigations on mechanical and tribological behaviour of particulate filled glass fabric reinforced epoxy composites. *J. Miner. Mater. Charact. Eng.* **1**(4), 160–167 (2013)
20. Akram, W.; Chaturvedi, S.K.; Ali, S.M.: Comparative study of mechanical properties of e-glass/epoxy composite materials with Al₂O₃, CaCO₃, SiO₂ AND PBO fillers. *Int. J. Eng. Res. Tech.* **2**(7), 1029–1034 (2013)



21. Abdalrazaq, I.; Abd Soud, W.; Abdullah, O.S.: Effects of different types of ceramic fillers on wear characteristics of glass fibres-epoxy composite. *J. Eng. Dev.* **17**(6), 164–174 (2013)
22. Gafsi, N.; Smaoui, I.; Verdejo, R.; Kharrat, M.; Manchado, M.Á.; Dammak, M.: Tribological and mechanical characterization of epoxy/graphite composite coatings: effects of particles' size and oxidation. *Proc. Inst. Mech. Eng. J: J. Eng. Tribol.* **235**(1), 129–137 (2021)
23. Chelliah, A.: Mechanical properties and abrasive wear of different weight percentage of TiC filled basalt fabric reinforced epoxy composites. *Mater. Res.* **22**(2), e20180431 (2019)
24. Hariprasad, P.; Kannan, M.; Ramesh, C.; Felix Sahayaraj, A.; Jenish, I.; Hussain, F.; Suresh, V.: [Retracted] mechanical and morphological studies of sansevieria trifasciata fiber-reinforced polyester composites with the addition of SiO₂ and B₄C. *Adv Mater Sci Eng* **2022**(1), 1634670 (2022)
25. Zhang, X.R.; Pei, X.Q.; Wang, Q.H.: Friction and wear studies of polyimide composites filled with short carbon fibers and graphite and micro SiO₂. *Mater. Des.* **30**(10), 4414–4420 (2009)
26. Suresha, B.; Chandramohan, G.; Sadananda Rao, P.R.; Sampathkumar, P.; Seetharamu, S.: Influence of SiC filler on mechanical and tribological behavior of glass fabric reinforced epoxy composite systems. *J. Reinf. Plast. Compos.* **26**(6), 565–578 (2007)
27. Nayak, R.K.; Dash, A.; Ray, B.C.: Effect of epoxy modifiers (Al₂O₃/SiO₂/TiO₂) on mechanical performance of epoxy/glass fiber hybrid composites. *Procedia Mater. Sci.* **6**, 1359–1364 (2014)
28. Zal, V.; Sadooghi, A.; Hashemi, S.J.; Rahmani, K.; Roohi, A.H.; Khodayari, H.; Babazadeh, J.: Experimental study of polyester/fiberglass/stainless steel fiber metal laminates mechanical properties. *Arab. J. Sci. Eng.* **49**, 11167–11179 (2024)
29. Rahmani, K.; Wheatley, G.; Sadooghi, A.; Hashemi, S.J.; Babazadeh, J.: The experimental investigation of hardness and wear behaviors of inner surface of the resin tubes reinforced by fibers. *Results Eng.* **11**, 100273 (2021)
30. Hashemi, S.J.; Sadooghi, A.; Rahmani, K.; Davarzani, F.; Akbari, S.: Investigation on the mechanical behavior of fiber-metal laminates based on polyvinyl chloride reinforced by 3D glass fibers. *Mater. Today Commun.* **25**, 101273 (2020)
31. Zhang, W.: Tribology of SiC ceramics under lubrication: features, developments, and perspectives. *Curr. Opin. Solid State Mater. Sci.* **26**(4), 101000 (2022)
32. Zhang, W.: A review of tribological properties for boron carbide ceramics. *Prog. Mater. Sci.* **116**, 100718 (2021)
33. Celik, A.; Lazoglu, I.; Kara, A.; Kara, F.: Investigation on the performance of SiAlON ceramic drills on aerospace grade CFRP composites. *J. Mater. Process. Technol.* **223**, 39–47 (2015)
34. Lukács, T.; Pereszlai, C.; Geier, N.: Delamination measurement in glass fibre reinforced polymer (GFRP) composite based on image differencing. *Composite Part B: Eng.* **248**, 110381 (2023)
35. Abd-Elwahed, M.S.: Drilling process of GFRP composites: modeling and optimization using hybrid ANN. *Sustainability* **14**(11), 6599 (2022)
36. Khashaba, U.A.; Abd-Elwahed, M.S.; Najjar, I.; Melaibari, A.; Ahmed, K.I.; Zitoune, R.; Eltahir, M.A.: Heat-affected zone and mechanical analysis of GFRP composites with different thicknesses in drilling processes. *Polymers* **13**(14), 2246 (2021)
37. Liu, L.; Qi, C.; Wu, F.; Zhang, X.; Zhu, X.: Analysis of thrust force and delamination in drilling GFRP composites with candle stick drills. *Int. J. Adv. Manuf. Technol.* **95**, 2585–2600 (2018)
38. Jessy, K.; Satish Kumar, S.; Dinakaran, D.; Seshagiri Rao, V.: Influence of different cooling methods on drill temperature in drilling GFRP. *Int. J. Adv. Manuf. Technol.* **76**, 609–621 (2015)
39. Tian, J.; Wu, F.; Zhang, P.; Lin, B.; Liu, T.; Liu, L.: The coupling effect and damage analysis when drilling GFRP laminates using candlestick drills. *Int. J. Adv. Manuf. Technol.* **102**, 519–531 (2019)
40. Erturk, A.T.; Vatanserver, F.; Yasar, E.; Guven, E.A.; Sinmazcelik, T.: Effects of cutting temperature and process optimization in drilling of GFRP composites. *J. Compos. Mater.* **55**(2), 235–249 (2021)
41. Mohan, N.S.; Ramachandra, A.; Kulkarni, S.M.: Influence of process parameters on cutting force and torque during drilling of glass-fiber polyester reinforced composites. *Compos. Struct.* **71**(3–4), 407–413 (2005)
42. Khashaba, U.A.; El-Sonbaty, I.A.; Selmy, A.I.; Megahed, A.A.: Drilling analysis of woven glass fiber-reinforced/epoxy composites. *J. Compos. Mater.* **47**(2), 191–205 (2013)
43. Natarajan, E.; Markandan, K.; Sekar, S.M.; Varadaraju, K.; Nesapan, S.; Albert Selvaraj, A.D.; Franz, G.: Drilling-induced damages in hybrid carbon and glass fiber-reinforced composite laminate and optimized drilling parameters. *J. Compos. Sci.* **6**(10), 310 (2022)
44. Kharat, W.S.; Sidhu, J.S.: Development of epoxy based composites filled with boron carbide (B₄C), tungsten disulphide (WS₂) and evaluation of its mechanical properties. *Int. J. Mech. Eng. Res.* **6**, 19–30 (2016)
45. Baptista, R.; Mendão, A.; Rodrigues, F.; Figueiredo-Pina, C.G.; Guedes, M.; Marat-Mendes, R.: Effect of high graphite filler contents on the mechanical and tribological failure behavior of epoxy matrix composites. *Theor. Appl. Fract. Mech.* **85**, 113–124 (2016)
46. Yasmin, A.; Daniel, I.M.: Mechanical and thermal properties of graphite platelet/epoxy composites. *Polymer* **45**(24), 8211–8219 (2004)
47. Shivamurthy, B.; Bhat, K.U.; Anandhan, S.: Mechanical and sliding wear properties of multi-layered laminates from glass fabric/graphite/epoxy composites. *Mater. Des.* **44**, 136–143 (2013)
48. Abenojar, J.; Martínez, M.A.; Velasco, F.; Pascual-Sánchez, V.; Martín-Martínez, J.M.: Effect of boron carbide filler on the curing and mechanical properties of an epoxy resin. *J. Adhes.* **85**(4–5), 216–238 (2009)
49. Bhagat, S.; Verma, P.K.: Effect of graphite filler on mechanical behavior of epoxy composites. *Int. J. Emerg. Tech. Adv. Eng.* **3**(2), 427–430 (2013)
50. Bhatia, S.; Khan, S.; Angra, S.: Effect of the content of silane-functionalized boron carbide on the mechanical and wear performance of B₄C reinforced epoxy composites. *High Perform. Polym.* **33**(10), 1165–1180 (2021)
51. Sudheer, M.; Hemanth, K.; Raju, K.; Bhat, T.: Enhanced mechanical and wear performance of epoxy/glass composites with PTW/graphite hybrid fillers. *Procedia Mater. Sci.* **6**, 975–987 (2014)
52. Arun, A.; Singh, K.K.: Friction and wear behaviour of glass fibre reinforced polymer composite (GFRP) under dry and oil lubricated environmental conditions. *Mater. Today: Proc.* **4**, 7285–7292 (2017)
53. Kim, S.S.; Shin, M.W.; Jang, H.: Tribological properties of short glass fiber reinforced polyamide 12 sliding on medium carbon steel. *Wear* **274–275**, 34–42 (2012)
54. Tasyurek, M.; Duzcukoglu, H.: Improving the wear behavior of epoxy resin with boron carbide reinforcement. *Iran. Polym. J.* **31**, 169–184 (2022)
55. Karthik, K.; Manimaran, A.: Wear behaviour of ceramic particle reinforced hybrid polymer matrix composites. *Int. J. Ambient Energ.* **41**(14), 1608–1612 (2020)
56. Çetkin, E.; Demir, M.E.; Ergün, R.K.: The effect of different fillers, loads, and sliding distance on adhesive wear in woven e-glass fabric composites. *Proc. Inst. Mech. Eng., Part E: J. Process Mech. Eng.* **237**(2): 418–429 (2023).
57. Suresha, B.; Seetharamu, S.; Kumaran, P.S.: Investigations on the influence of graphite filler on dry sliding wear and abrasive wear behaviour of carbon fabric reinforced epoxy composites. *Wear* **267**, 1405–1414 (2009)



58. Parasuraman, S.; Elamvazuthi, I.; Kanagaraj, G.; Natarajan, E.; Pugazhenthii, A.: Assessments of process parameters on cutting force and surface roughness during drilling of AA7075/TiB₂ in situ composite. *Materials* **14**(7), 1726 (2021)
59. Bayraktar, Ş; Turgut, Y.: Investigation of the cutting forces and surface roughness in milling carbon fiber reinforced polymer composite material. *Mater. Technol.* **50**(4), 591–600 (2016)
60. Melentiev, R.; Priarone, P.C.; Robiglio, M.; Settineri, L.: Effects of tool geometry and process parameters on delamination in CFRP drilling. An overview *Procedia Cirp* **45**, 31–34 (2016)
61. Krishnaraj, V.; Prabukarthi, A.; Ramanathan, A.; Elanghovan, N.; Kumar, M.S.; Zitoune, R.; Davim, J.P.: Optimization of machining parameters at high speed drilling of carbon fiber reinforced plastic (CFRP) laminates. *Compos. Part B: Eng.* **43**(4), 1791–1799 (2012)
62. Sunny, T.; Babu, J.; Philip, J.: Experimental studies on effect of process parameters on delamination in drilling GFRP composites using taguchi method. *Procedia Mater. Sci.* **6**, 1131–1142 (2014)
63. Ghasemi, F.A.; Hyvadi, A.; Payganeh, G.; Arab, N.B.M.: Effects of drilling parameters on delamination of glass epoxy composites. *Aust. J. Basic Appl. Sci.* **5**(12), 1433–1440 (2011)
64. Ramesh, B.N.; Suresha, B.: Optimization of tribological parameters in abrasive wear mode of carbon-epoxy hybrid composites. *Mater. Des.* **59**, 38–49 (2014)
65. Latha, P.S.; Rao, M.V.: Investigation into effect of ceramic fillers on mechanical and tribological properties of bamboo-glass hybrid fiber reinforced polymer composites. *SILICON* **10**, 1543–1550 (2018)
66. Suresha, B.; Chandramohan, G.; Mohanram, P.V.: Role of fillers on three-body abrasive wear behavior of glass fabric reinforced epoxy composites. *Polym. Compos.* **30**(8), 1106–1113 (2009)
67. Basavarajappa, S.; Ellangovan, S.: Dry sliding wear characteristics of glass-epoxy composite filled with silicon carbide and graphite particles. *Wear* **296**(1–2), 491–496 (2012)

